

Spontaneous decay of excited atomic states near a carbon nanotube

I. V. Bondarev, G. Ya. Slepian and S. A. Maksimenko

The Institute for Nuclear Problems, The Belarusian State University, Bobruiskaya Str.11, 220050 Minsk, BELARUS

Spontaneous decay process of an excited atom placed inside or outside (near the surface) a carbon nanotube is analyzed. Calculations have been performed for various achiral nanotubes. The effect of the nanotube surface has been demonstrated to dramatically increase the atomic spontaneous decay rate – by 6 to 7 orders of magnitude compared with that of the same atom in vacuum. Such an increase is associated with the nonradiative decay via surface excitations in the nanotube.

Theoretical prediction of the Purcell effect in 1946 [1] has stimulated series of works, both theoretical and experimental, aimed at the detailed investigation of the phenomenon (see recent papers [2, 3, 4, 5, 6] and references therein). The effect lies in the fact that the spontaneous decay rate of an excited atom essentially depends on whether or not the atom is located near optical inhomogeneities and interfaces of media with differing optical properties. Depending on the specific configuration of inhomogeneities (interfaces), the atomic spontaneous decay rate may both increase and decrease compared with that of the same atom in free space. The Purcell effect took on special significance recently in view of rapid progress in physics of low-dimensional nanostructures. It was shown to be of great importance for microcavities [2], optical fibers [3], photonic crystals [4], semiconductor quantum dots [7].

In Ref. [6], it was first suggested on the basis of the model of an ideally conducting cylinder that spontaneous decay process of excited atomic states near a carbon nanotube (CN) might possess nontrivial peculiarities. However, the ideally conducting cylinder is not quite an adequate model to describe the optic properties of real CNs. It is our purpose in the present paper to give consistent consideration to spontaneous decay processes of the excited atom in the vicinity of CNs. We calculate atomic spontaneous decay rate variation for infinitely long achiral single-wall CNs of different radii and demonstrate that the decay rate may dramatically increase due to the nonradiative decay via CN surface excitations.

Quantum theory of the spontaneous decay of excited atomic states in the vicinity of CN requires the solution of two fundamental problems. They are (i) the problem of the macroscopic description of the optical properties of solitary CN and (ii) the quantization problem of an electromagnetic field in the presence of CN. We solve problem (i) based upon the model described in Refs. [8, 9]. According to that model, CN is changed by the infinitely thin anisotropically conducting cylinder with effective boundary conditions imposed in such a way that the field at a distance from the cylinder surface be identical to the actual electromagnetic field excited in the system. In so doing, only the axial conductivity of CN is taken into account and the transverse conductivity is neglected for the following reason. The axial conductivity forms by intraband and direct interband transitions of π -electrons in CN, while the transverse one only forms by indirect interband transitions [10, 11]. The intraband transitions dominate at lower frequencies and the interband ones start essentially contributing to the total CN conductivity at higher frequencies. However, the contribution of the indirect interband transitions, being strongly suppressed by depolarization fields, is always smaller compared with that of the direct interband transitions [10, 11]. We use the dispersion law for π -electrons in the tight-binding approximation with allowance made for the azimuthal momentum quantization. Energy dissipation is taken into account within the relaxation time approximation. The spatial dispersion of the CN conductivity is neglected (see Refs. [8, 9] for its role in CNs).

The quantization procedure of the electromagnetic field, problem (ii), faces difficulties similar to those in quantum optics of 3D Kramers-Kronig media where the canonical quantization scheme commonly used does not work since, because of absorption, the respective operator Maxwell equations become non-Hermitian. A standard approach overcoming these difficulties involves a noise current term incorporated into the operator Maxwell equations [12]. We use the analogous approach to quantize the electromagnetic field in the presence of CN. In this case, the noise current becomes the surface one and, therefore, may be incorporated into the boundary conditions for the Maxwell equations rather than into the Maxwell equations themselves. As this takes place, the effective boundary conditions for electric field and magnetic field operators in frequency-domain space take the form

$$\begin{aligned} \mathbf{n} \times \left(\hat{\mathbf{E}} \Big|_{r=R_{cn}+0} - \hat{\mathbf{E}} \Big|_{r=R_{cn}-0} \right) &= 0, \\ \mathbf{n} \times \left(\hat{\mathbf{H}} \Big|_{r=R_{cn}+0} - \hat{\mathbf{H}} \Big|_{r=R_{cn}-0} \right) + \frac{4\pi}{c} \hat{J}_z^N \mathbf{e}_z &= \frac{4\pi}{c} \sigma_{zz}(\omega) \hat{E}_z \mathbf{e}_z, \end{aligned} \quad (1)$$

where r is the radial spatial coordinate, R_{cn} the CN radius, \mathbf{n} and \mathbf{e}_z are the unit vectors along the external normal to the CN surface and along the CN axis, respectively, $\sigma_{zz}(\omega)$ is the axial dynamical conductivity of CN (see Eq.(36) in Ref. [8]), \hat{J}_z^N is the axial noise current operator. The latter one is expressed in terms of 2D scalar bosonic field

operator $\hat{f}(\mathbf{R})$ ($\mathbf{R} \in \text{CN}$ surface) as $\hat{J}_z^N = \sqrt{\hbar\omega \text{Re} \sigma_{zz}(\omega)/\pi} \hat{f}(\mathbf{R})$ and is responsible for correct commutation relations of $\hat{\mathbf{E}}$ and $\hat{\mathbf{H}}$ operators [12]. Homogeneous Maxwell equations along with boundary conditions (1) describe quantum electrodynamics of CNs.

Let the excited atom with an electric dipole transition allowed be located in the vicinity of CN and let the atomic dipole moment be oriented along the CN axis. Following the quantization scheme above, one can by analogy with Ref. [2] obtain the Volterra integral equation for atomic decay dynamics from the upper stationary state to the lower one

$$C_u(t) = 1 + \int_0^t K(t-t') C_u(t') dt' \quad (2)$$

with C_u being the occupation probability amplitude of the upper state and the kernel given by

$$K(\tau) = \frac{4k_A^2 |\mu_z|^2}{\hbar} \int_0^\infty d\omega \frac{\text{Im} G_{zz}(\mathbf{r}_A, \mathbf{r}_A, \omega)}{i(\omega - \omega_A)} \left[e^{-i(\omega - \omega_A)\tau} - 1 \right], \quad (3)$$

where μ_z and ω_A are the matrix element and the frequency of the atomic dipole transition, respectively, \mathbf{r}_A is the radius-vector of the atomic position, $k_A = \omega_A/c$, and $G_{zz}(\mathbf{r}, \mathbf{r}_A, \omega)$ is the axial component of the classical electromagnetic field Green tensor in the presence of CN.

For further calculations we need Green tensor components $G_{\alpha z}$ ($\alpha = r, \varphi, z$ are the cylindrical coordinates associated with CN). We use the representation $G_{\alpha z} = (k^{-2} \partial_\alpha \partial_z + \delta_{\alpha z}) g$ with $g(\mathbf{r}, \mathbf{r}_A, \omega)$ being the scalar Green function of the electromagnetic field in the presence of CN. The latter one is expanded over cylindrical waves in terms of boundary conditions (1), so that at $r, r_A > R_{cn}$ one obtains

$$g = g_0 - \frac{R_{cn}}{(2\pi)^2} \sum_{p=-\infty}^{\infty} e^{ip\varphi} \int_C \frac{\beta(\omega) v^2 I_p^2(vR_{cn}) K_p(vr_A) K_p(vr)}{1 + \beta(\omega) v^2 R_{cn} I_p(vR_{cn}) K_p(vR_{cn})} e^{ihz} dh, \quad (4)$$

where $g_0 = \exp(ik|\mathbf{r} - \mathbf{r}_A|)/4\pi|\mathbf{r} - \mathbf{r}_A|$ is the free space Green function, $\beta(\omega) = 4\pi i \sigma_{zz}(\omega)/\omega$, $v = \sqrt{h^2 - k^2}$, $I_p(X)$ and $K_p(X)$ are the modified cylindrical Bessel functions. Integration contour C goes along the real axis of the complex plane and envelopes branch points $\pm k$ from below and from above, respectively. For $r, r_A < R_{cn}$, Eq.(4) is modified by the replacement $I_p \leftrightarrow K_p$ in the numerator of the integrand.

Consider decay process in the Markovian approximation. Then, factor $[\exp(-ix\tau) - 1]/ix$ in Eq.(3) is changed by $\pi\delta(x) + i\mathcal{P}(1/x)$ (\mathcal{P} denotes the principal value), and one arrives at the exponential decay model with $K(\tau) = -\Gamma/2 + i\delta\omega$, where Γ and $\delta\omega$ are the decay rate and the Lamb shift of the upper atomic level, respectively. For the outward atomic position ($r_A > R_{cn}$), the decay rate is written in view of Eqs.(2)-(4) as

$$\frac{\Gamma}{\Gamma_0} = \xi(\omega_A) = 1 + \frac{3R_{cn}}{2\pi k_A^3} \sum_{p=-\infty}^{\infty} \int_C \frac{\beta_A v_A^4 I_p^2(v_A R_{cn}) K_p^2(v_A r_A)}{1 + R_{cn} \beta_A v_A^2 I_p(v_A R_{cn}) K_p(v_A R_{cn})} dh, \quad (5)$$

with $\beta_A = \beta(\omega_A)$, $v_A = \sqrt{h^2 - k_A^2}$, $\Gamma_0 = 4k_A^3 |\mu_z|^2/3\hbar$ being the free space decay rate and $\xi(\omega_A)$ representing the influence of CN. For the inward position ($r_A < R_{cn}$), Eq.(5) is modified by the simple replacement $r_A \leftrightarrow R_{cn}$ in the numerator of the integrand. Note the divergence of the integral in Eq.(5) at $r_A = R_{cn}$, i. e. when the atom is located directly on the CN surface. This divergence originates from the averaging procedure over physically infinitely small volume when describing CN optical properties. Such an averaging does not assume any additional atoms on the CN surface, to take them into consideration the procedure must be modified. Thus, the applicability domain of our model is restricted by the condition $|r_A - R_{cn}| > a$, where $a = 1.42 \text{ \AA}$ is the interatomic distance in CN.

The decay of the excited atom interacting with medium may proceed both via real photon emission (radiative decay) and via virtual photon emission with subsequent medium quasiparticle excitation (nonradiative decay). Both of these decay channels are present in atomic spontaneous decay rate Γ described by Eq.(5). The problem of the total Γ partition to radiative and nonradiative contributions is not trivial. Radiative contribution Γ_r was estimated by using a Poynting vector approach for the atom near a microsphere in [2] and for the atom inside an optic fiber in [3]. Following this approach, we estimate the spontaneous radiation intensity distribution $I(\mathbf{r}, t) = |\mathbf{F}(\mathbf{r}, \mathbf{r}_A, \omega_A)|^2 \exp(-\Gamma t)$, where

$$F_\alpha(\mathbf{r}, \mathbf{r}_A, \omega_A) = -4\pi i k_A^2 \mu_z \left\{ G_{\alpha z}(\mathbf{r}, \mathbf{r}_A, \omega_A) - \frac{1}{\pi} \mathcal{P} \int_0^\infty \frac{\text{Im} G_{\alpha z}(\mathbf{r}, \mathbf{r}_A, \omega)}{\omega + \omega_A} d\omega \right\},$$

at large distances $|\mathbf{r}| \rightarrow \infty$. In so doing, the second term does not contribute and the contribution of the first term is easily found by the stationary phase method [13] to give in the spherical coordinates ($|\mathbf{r}|, \phi, \theta$) associated with the

atom

$$\lim_{|\mathbf{r}| \rightarrow \infty} \mathbf{F}(\mathbf{r}, \mathbf{r}_A, \omega_A) \simeq -ik_A^2 \mu_z \frac{e^{ik_A |\mathbf{r}|}}{|\mathbf{r}|} \mathbf{e}_\theta \sin \theta \sum_{p=-\infty}^{\infty} \Xi_p(-ik_A \sin \theta) e^{ip\phi}$$

with \mathbf{e}_θ being the spherical ort and

$$\Xi_p(X) = \begin{cases} \frac{I_p(Xr_A)}{1 + R_{cn} \beta_A X^2 I_p(XR_{cn}) K_p(XR_{cn})}, & \text{if } r_A < R_{cn} \\ I_p(Xr_A) - \frac{R_{cn} \beta_A X^2 I_p^2(XR_{cn}) K_p(Xr_A)}{1 + R_{cn} \beta_A X^2 I_p(XR_{cn}) K_p(XR_{cn})}, & \text{if } r_A > R_{cn}. \end{cases}$$

The relative contribution of the radiative decay is then given by

$$\begin{aligned} \frac{\Gamma_r}{\Gamma} &= \frac{c}{2\pi\hbar\omega_A} \lim_{|\mathbf{r}| \rightarrow \infty} \int_0^\infty dt \int_0^{2\pi} d\phi \int_0^\pi |\mathbf{r}|^2 I(\mathbf{r}, t) \sin \vartheta d\vartheta \\ &= \frac{3}{4\xi(\omega_A)} \sum_{p=-\infty}^{\infty} \int_0^\pi |\Xi_p(-ik_A \sin \vartheta)|^2 \sin^3 \vartheta d\vartheta. \end{aligned} \quad (6)$$

Figure 1 shows the results of the numerical calculations of factor $\xi(\omega_A)$ according to Eq.(5) for metallic and semiconducting CNs of $(m, 0)$ type ("zigzag"). The atom is located on the symmetry axis inside CN. The presence of CN is seen to drastically accelerate spontaneous decay process of an excited atomic state. Frequency range $0.305 < \hbar\omega_A/2\gamma_0 < 0.574$ ($\gamma_0 = 2.7$ eV is the carbon overlap integral) corresponds to visible light. Lower frequencies $\hbar\omega_A/2\gamma_0 < 0.305$ correspond to infra-red waves emitted by highly excited Rydberg atomic states. At these frequencies, the large difference (3–4 orders of magnitude) is seen in the value of $\xi(\omega_A)$ for metallic ($m = 3q$, $q = 1, 2, \dots$) and semiconducting ($m \neq 3q$) CNs. The difference is caused by the Drude-type conductivity (intraband electronic transitions) dominating in this region, whose relative contribution to the total CN conductivity is larger in metallic CNs than in semiconducting ones [8, 9, 10, 11]. As the frequency increases, interband electronic transitions start manifesting themselves and function $\xi(\omega_A)$ becomes irregular. At high frequencies, there is no significant difference between metallic and semiconducting CNs of close radii. Function $\xi(\omega_A)$ has dips when ω_A equals the interband transition frequencies; in particular, there is a dip at $\hbar\omega_A = 2\gamma_0$ for all CNs considered. It is essential that $\xi(\omega_A) \gg 1$ throughout the entire frequency range considered. This lets us formulate the central result of the present paper: *the spontaneous decay probability of the atom in the vicinity of CN is larger by a few orders of magnitude than that of the same atom in free space.* In other words, the Purcell effect is extraordinarily strong in CNs. This is physically explained by the photon vacuum renormalization: the density of photonic states (and, as a consequence, the atomic decay rate) near CN effectively increases ($\rho^{eff}(\omega) d\omega = \xi(\omega) \omega^2 d\omega / \pi c^3$) since, along with ordinary free photons, there appear the photonic states coupled with CN electronic quasiparticle excitations.

In Refs. [8, 9], the possibility was shown of the existence of slow surface electromagnetic waves in CNs. In Ref. [2], such waves were shown to be responsible for the strong Purcell effect for the atom in the spherical microcavity. The results of the present paper agree qualitatively with those obtained in Ref. [2]. Quantitatively, $\xi_{max} \sim 10^6 - 10^7$ for CNs while $\xi_{max} \sim 10^4$ for the microcavity [2], i. e. the Purcell effect is much stronger in CNs. It is worth noting that for the atoms with large enough Γ_0 , there is the risk of going beyond the applicability limits of the two-level model and Markovian approximation. Then, in the first case, the mutual overlap is possible of the levels due to their strong broadening and, in the second one, the atomic spontaneous decay may become nonexponential so that the problem may require the numerical solution of integral equation (2) with kernel (3).

Figure 2 shows $\xi(\omega_A)$ for the atom located outside CN at different distances from the CN surface. The qualitative behavior of $\xi(\omega_A)$ is similar to that represented in Figure 1 for the atom inside CN. Factor $\xi(\omega_A)$ is seen to rapidly decrease with raising the distance as it should be in view of the evident fact that photonic states coupled with CN electronic excitations (those increasing effective density $\rho^{eff}(\omega)$) are spatially localized on the CN surface and their coupling strength with the excited atom decreases with raising the distance of the atom from CN.

Figure 3 shows the ratio Γ_r/Γ calculated according to Eq.(6) for the atom in the centre of different CNs. (Note that $\Gamma_r/\Gamma = W_s(\omega_A)/\hbar\omega_A$ with $W_s(\omega_A)$ being the total power of the atomic spontaneous radiation far from CN.) The ratio is very small indicating that the nonradiative decay dominates. However, the radiative decay is seen to essentially contribute in the vicinity of the interband transition frequencies so that the frequency dependence of $W_s(\omega_A)$ (which, in principle, can be measured experimentally) reproduces CN electronic structure peculiarities. The main conclusion one can draw from Figure 3 is *the Purcell effect in CNs, along with the increase of the atomic spontaneous decay rate, manifests itself by decreasing the power of the spontaneous radiation.*

Our model of the atomic spontaneous decay in the presence of CN includes, as a limiting case, the model of the ideally conducting cylinder considered in Ref. [6]. In particular, our Eq.(5) reduces for the outward atomic position to Eqs.(15),(18) of Ref. [6] as $\sigma_{zz} \rightarrow \infty$. The inset in Figure 2 shows factor $\xi(\omega_A)$ at $\omega_A = 3\gamma_0/\hbar$ ($k_A R_{cn} \simeq 0.01$) as a function of r_A/R_{cn} for this case. The dependence is similar to that reported in Ref. [6] for z-oriented dipole at $k_A R_{cn} = 1$. For the atom inside CN, Eq.(5) yields $\xi(\omega_A) \rightarrow 0$ as $\sigma_{zz} \rightarrow \infty$ — the result is natural since in this case only one eigen electromagnetic mode can propagate in CN; this mode is essentially transverse and, consequently, is not coupled with the atomic dipole moment oriented longitudinally. However, the actual $\xi(\omega_A)$ behavior discussed above is quite different from that predicted by the ideally conducting cylinder model since the latter one does not account for CN electronic quasiparticle excitations responsible for the nonradiative atomic decay dominating the total spontaneous decay process.

Our theory may be generalized to cover the transverse atomic electric dipole orientation, electric quadrupole and magnetic dipole atomic transitions, properties of organic molecules inside/outside CNs [14] and of fullerene peapods [15]. The mechanism revealed of the photon vacuum renormalization is likely to manifest itself in other phenomena in CNs such as, for example, Casimir forces, electromagnetic fluctuations, etc. [16].

The results of the present work may be tested by methods of atomic fluorescent spectroscopy and may possess various physical consequences. In particular, the effect of the drastic increase of the atomic spontaneous decay rate may turn out to be of practical importance in problems of the laser control of atomic motion [17], yielding the increase of the ponderomotive force acting on the atom moving in the vicinity of CN in a laser field. One might expect the Purcell effect peculiarities that we predict for CNs to manifest in macroscopic anisotropically conducting waveguides with strong wave deceleration (for example, in microwave spiral or collar waveguides with highly excited Rydberg atoms inside).

The work was financially supported by the Foundation for Basic Research of the National Academy of Sciences of the Republic of Belarus (Grants No F01-176 and No F02R-047).

-
- [1] E. M. Purcell, Phys. Rev. **69**, 681 (1946).
 - [2] H. T. Dung, L. Knöll and D.-G. Welsch, Phys. Rev. A **64**, 013804 (2001); H. T. Dung, L. Knöll and D.-G. Welsch, *ibid.* **62**, 053804 (2000).
 - [3] T. Sondergaard and B. Tromborg, Phys. Rev. A **64**, 033812 (2001).
 - [4] Y. Yang and S.-Y. Zhy, Phys. Rev. A **62**, 013805 (2000).
 - [5] *Mesoscopic Physics and Electronics*, eds. T. Ando, T. Arakawa, K. Furuya, S. Komiyama and H. Nakashima (Springer, Berlin, 1998).
 - [6] V. V. Klimov and M. Ducloy, Phys. Rev. A **62**, 043818 (2000).
 - [7] M. Sugawara, Phys. Rev. B **51**, 10743 (1995); E. Hanamura, *ibid.* **38**, 1228 (1988); D. G. Deppe et al., IEEE J. Quant. El. **35**, 1238 (1999); D. G. Deppe et al., IEEE J. Quant. El. **35**, 1502 (1999); M. Pelton and Y. Yamamoto, Phys. Rev. A **59**, 2418 (1999); O. Benson and Y. Yamamoto, *ibid.* **59**, 4756 (1999).
 - [8] G. Ya. Slepyan, S. A. Maksimenko, A. Lakhtakia, O. Yevtushenko and A. V. Gusakov, Phys. Rev. B **60**, 17136 (1999).
 - [9] S. A. Maksimenko and G. Ya. Slepyan, in: *Electromagnetic Fields in Unconventional Structures and Materials*, eds. O. N. Singh and A. Lakhtakia (Wiley, New York, 2000), p. 217.
 - [10] S. Tasaki, K. Maekawa and T. Yamabe, Phys. Rev. B **57**, 9301 (1998).
 - [11] R. Saito and H. Kataura, in *Carbon Nanotubes*, eds. M. S. Dresselhaus, G. Dresselhaus and Ph. Avouris (Springer, Berlin, 2001), p. 216.
 - [12] W. Vogel, D.-G. Welsch and S. Wallentowitz, *Quantum Optics: an Introduction* (Wiley-VCH, New York, 2001).
 - [13] R. B. Dingle, *Asymptotic Expansions: Their Derivation and Interpretation* (Academic Press, London, 1973).
 - [14] E. P. Petrov, V. N. Bogomolov, I. I. Kalosha, and S. V. Gaponenko, Phys. Rev. Lett. **81**, 77 (1998).
 - [15] X. Liu, T. Pichler, M. Knupfer et. al., Phys. Rev. B **65**, 045419 (2002).
 - [16] M. Bordag, U. Mohideen, and V. M. Mostepanenko, Phys. Rep. **353**, 1 (2001).
 - [17] M. O. Scully and M. S. Zubairy, *Quantum Optics* (Cambridge Univ. Press, Cambridge, 2001).

Figure captions:

Figure 1: Factor $\xi(\omega_A)$ calculated from Eq.(5) for the atom in the center of different "zigzag" CNs. Surface axial conductivities σ_{zz} appearing in Eq.(5) were calculated in the τ -approximation with $\tau = 3 \times 10^{-12} \text{ s}^{-1}$.

Figure 2: Factor $\xi(\omega_A)$ for the atom at different distances outside "zigzag" (9,0) CN. Inset: $\xi(\omega_A)$ at $\omega_A = 3\gamma_0/\hbar$ as a function of r_A/R_{cn} for the atom near (9,0) CN in the model of the ideally conducting cylinder.

Figure 3: Ratio Γ_r/Γ calculated from Eq.(6) for the atom in the center of different "zigzag" CNs.

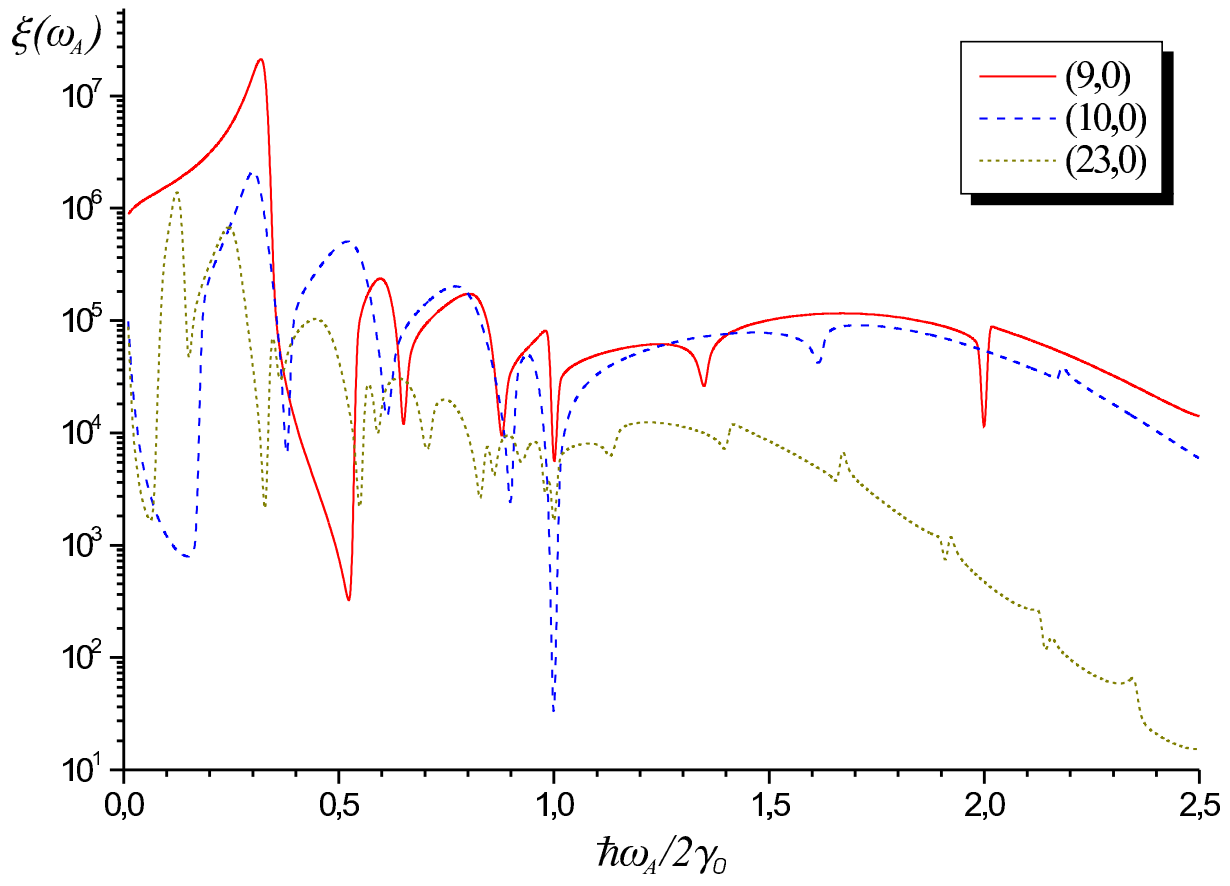


FIG. 1:

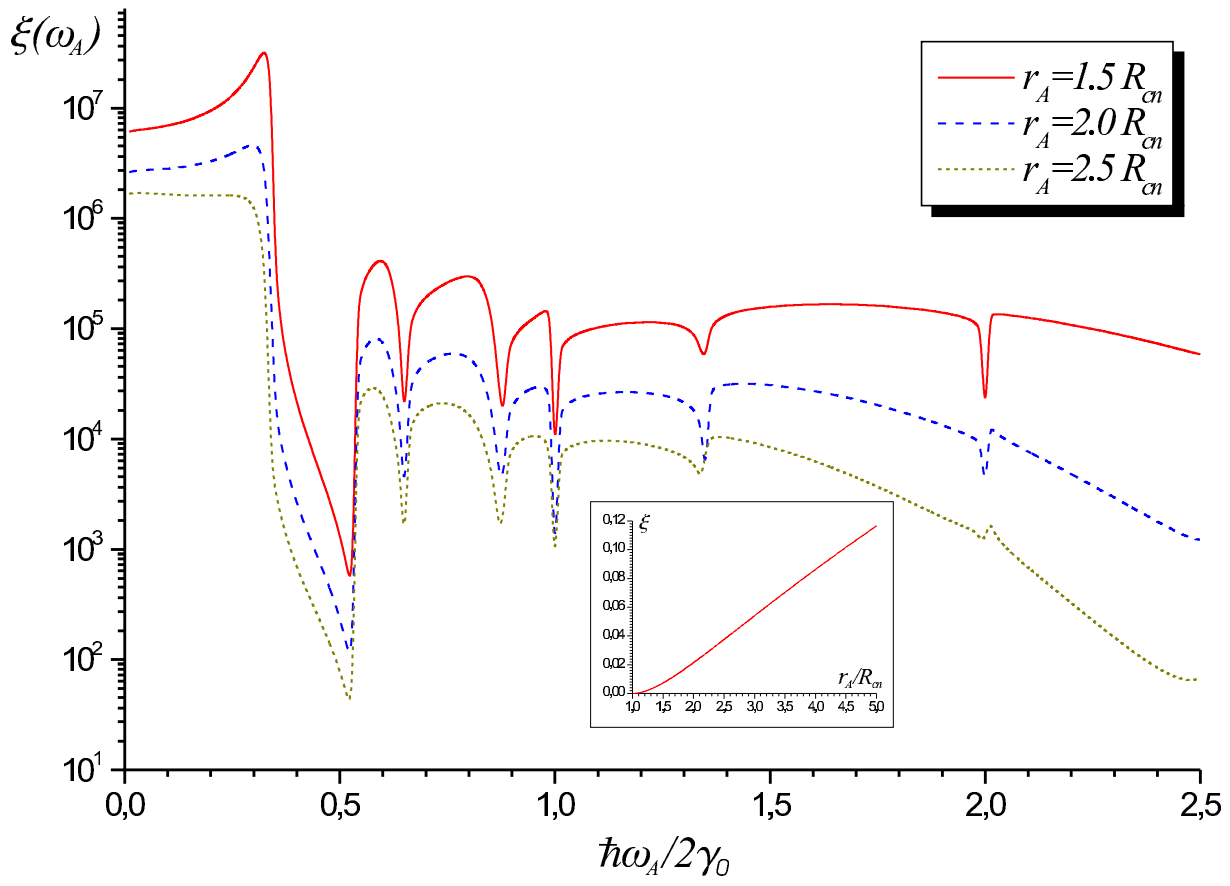


FIG. 2:

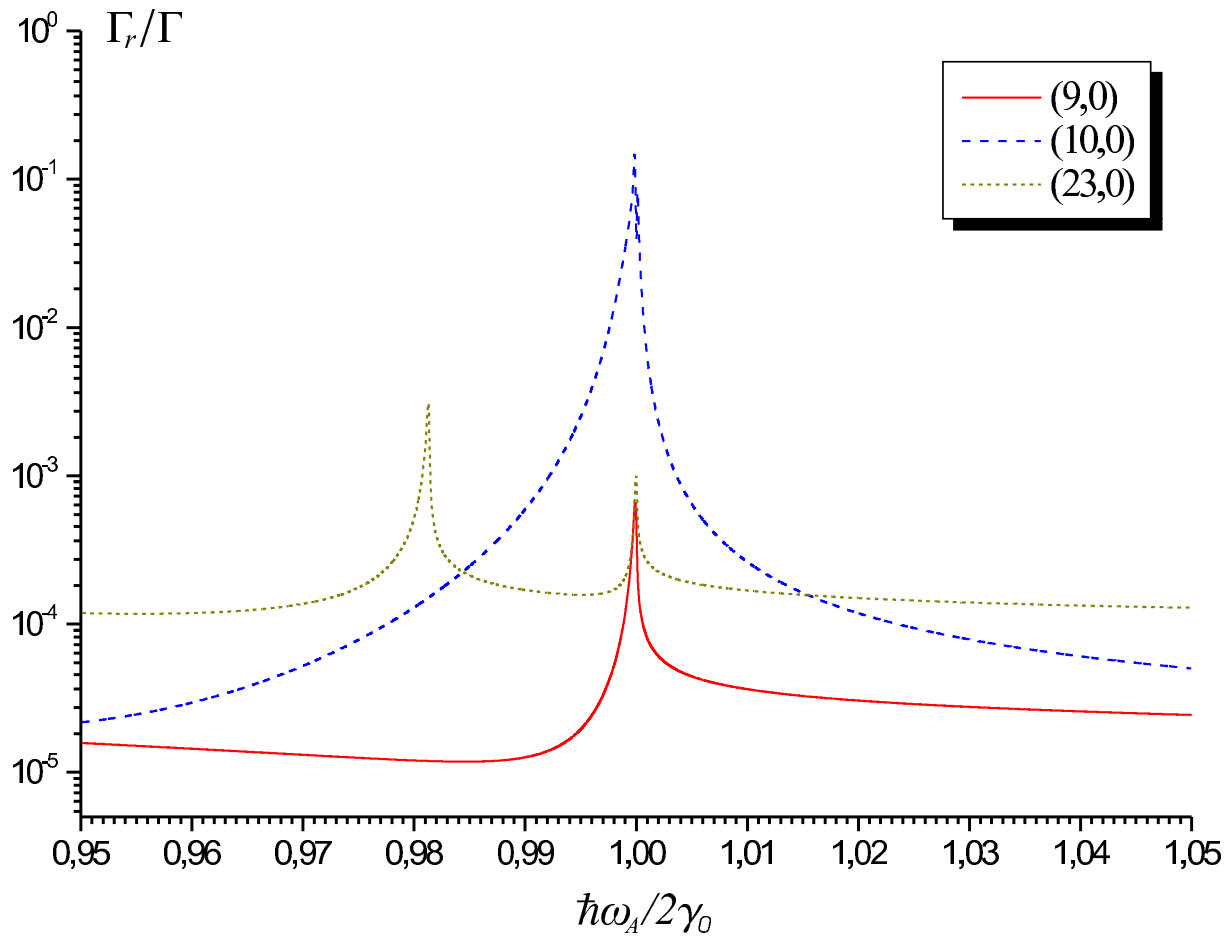


FIG. 3: